25 Gbit/s silicon based modulators for the 2 μm wavelength band

Wei Cao[1,*], Milos Nedeljkovic[1], Shenghao Liu[1], Callum G. Littlejohns[1], David J. Thomson[1], Frederic Gardes[1], Zhengqi Ren[1], Ke Li[1], Graham T. Reed[1], Goran Z. Mashanovich[1,3]

[1]: Optoelectronics Research Centre, University of Southampton, Southampton, Hampshire SO17 1BJ, United Kingdom
[2]: School of Electrical Engineering, University of Belgrade, 11120 Belgrade, Serbia
** email: wei.cao@soton.ac.uk*

Abstract: We demonstrate high-speed silicon modulators optimized for operating at the wavelength of 2 μm. The Mach-Zehnder interferometer carrier-depletion modulator has a modulation efficiency ($V_\pi \cdot L_\pi$) of 2.89 V·cm at 4 V reverse bias. It operates at a data rate of 25 Gbit/s with an extinction ratio of 6.25 dB.

OCIS codes: (130.4110) Modulators; (060.4080) Modulation; (060.4510) Optical communications; (130.0130) Integrated optics; (130.3120) Integrated optics devices; (250.0250) Optoelectronics.

1. Introduction

The approaching of the theoretical capacity limit of conventional single mode fibres (SMFs) [1] becomes much more imminent as the coherent detection gradually gains popularity. Hollow-core photonic bandgap fibres (HC-PBGF) however provide a tantalizing solution to surmount the so-called“capacity crunch” by offering lower predicted loss and nonlinearity than the best SMF. It does so by residing more mode into the hollow core, where filled with air or other gases. Therefore the theoretical lowest loss of such fibres shifts to 2 μm [2], which opens a new wavelength telecommunication window [3]. Coincidentally, such a wavelength aligns well with the gain spectrum of thulium-doped fibre amplifiers (TDFA). Moreover, widely used Silicon-on-Insulator (SOI) platform with 220nm Si top layer is largely compatible with 2 μm wavelength. Our group has previously demonstrated both 20 Gbit/s silicon photonics based detector and modulator at 2 μm [4] [5]. In this paper we present state-of-the art silicon photonics based high speed modulators operating at up to 25 Gbit/s with improved insertion loss and extinction ratio.

2. Design

Plasma dispersion effect in silicon at 1300 nm and 1550 nm has long been adopted in high-speed silicon modulators and the effect is stronger at 2 μm according to the prediction [6]. The modulator in our design uses a PN junction and the performance is optimized under reverse bias at 2 μm wavelength. The optimization is carried out as a series of simulations using both Silvaco TCAD tools for RF electrical field analysis and MATLAB [7] together with Lumerical Mode solutions for the optical mode calculation.

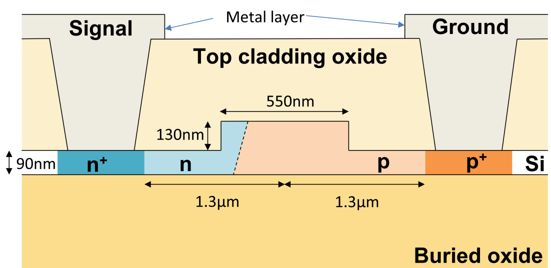

Fig. 1: The phase shifter cross section of the 2 μm MZI modulator.

The phase shifter exploit the carrier depletion effect, and as shown in Figure 1 it comprises a PN junction. Devices are fabricated on 220 nm SOI wafers with a 2 μm buried oxide (BOX) layer. The silicon rib waveguide is 550 nm wide and etched by 90 nm in the slab region. The n doping is implanted with self-aligning mask so the junction appears angled and positioned towards the n side. The self-alignment step helps reduce the junction position variation across devices introduced by the lithography [8]. The highly doped regions are 1.3 μm away from the junction. The target doping concentrations in the simulation are 3.8e17 cm^{-3}, 1.1e18 cm^{-3}, 1.5e17 cm^{-3}, 7.5e17 cm^{-3}, 1e20 cm^{-3} and 1e20 cm^{-3} for the p, n, p(rib), n(rib), p+, and n+ regions respectively. The

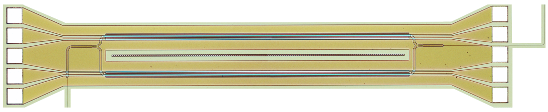

Fig. 2: MZM mask design for the stepper lithography.

Mach-Zehnder modulator contains two arms of the aforementioned phase shifter each with 2 mm length as shown in Figure 1. A travelling wave electrode is used to ensure co-propagate of RF and optical signals.

The device is fabricated in a CORNERSTONE multi-project wafer (MPW) run.

3. Experimental setup

The most 1310/1550 nm components in the original high-speed lab set-up is incompatible with the 2 μm wavelength. Therefore some dedicated 2 μm equipment has been used, as shown in Figure 3, these includes: A Thorlabs TLK-L1950R tunable laser (1890 nm - 2020 nm), an EOT ET-5000 high speed 2 μm InGaAs detector (with rated bandwidth of >12.5 GHz and peak responsivity of 1.3 A/W at 2000 nm); an amplified Thorlabs low speed 2 μm InGaAs detector; and Thorlabs SM2000 silica fibres. We have also made a bespoke TDFA to increase the optical power. As the seed tunable laser power is relatively low, we found out it works more favourably to place the TDFA before the device. During the RF characterisation, a Bit Pattern Generator (BPG) is used to generate a pseudorandom binary sequence (PRBS). The BPG is capable output 2 V peak-peak signal, so in the push-pull configuration no further RF amplifier is required. A bias tee is used to combine DC bias and high speed RF signal.

Compared to the conventional 1310/1550 nm setup, there are limitations in the 2 μm system. The high speed detector had a nominal bandwidth of >12.5GHz, limiting the speed at which we could measure the modulator to around 25 Gbit/s and with reduced extinction ratio.

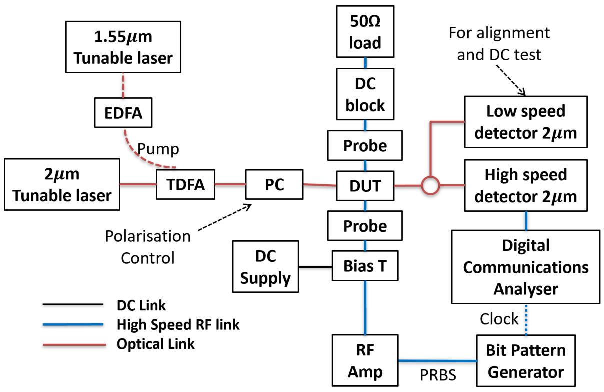

Fig. 3: High-speed RF measurement set up for 2 μm wavelength modulator.

4. Results

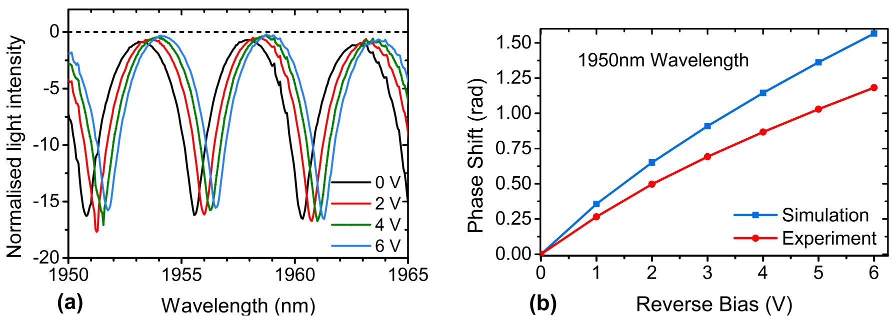

Fig. 4: (a) Normalised light intensity from the MZM under 0 -6V bias voltages. (b) Experimental and simulated phase shift for a MZI modulator with 0.2 cm long phase shifter.

The modulation efficiency ($V_\pi \cdot L_\pi$) at a reverse bias of 4 V is 2.89 V·cm at 1950 nm. The experimental phase shift for the measured MZM that comprises a 2.0 mm long phase shifter is shown in figure 4. The simulated phase shift is also shown in the same graph. It can be seen that the response agrees reasonably well with the simulation predictions. The discrepancy may be due to RF signal is attenuated too much towards the far end of the 2 mm travelling electrode.

The high speed RF characterization is carried out in a push-pull configuration. The DC bias is -4.5 V. An high-speed $2^7 - 1$ psuedorandom-bit-stream OOK signal directly output from BPG with a peak-to-peak amplitude of 2 V is applied on each arm. At 1956.5 nm, the device modulates at 10 Gbit/s with an extinction ratio of 12.7 dB, as in figure 5(a), at 20 Gbit/s the extinction ratio is 10.3 dB, as in figure 5(b), and at 25 Gbit/s the extinction ratio is 6.25 dB, as in figure 5(c). The insertion loss of the MZM with 2 mm phase shifter is 4.96dB, and a similar MZI without doping and metal is also tested to have a insertion loss of 1.25dB. Because of the bandwidth limit of the detector we were unable to obtain an eye diagram for data rates greater than 25 Gbit/s at 2 µm wavelength. We expect that the modulator can operate at higher data rates and given the decent extinction ratio, it is also worth to try PAM4 operations.

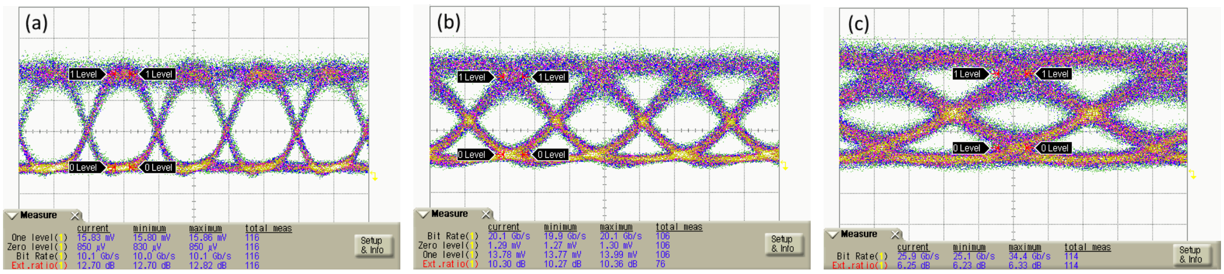

Fig. 5: Eye diagram for MZI modulator at 1956.5 nm wavelength. (a) Data rate is 10 Gb/s, Extinction ratio is 12.7 dB. (b) Data rate is 20 Gb/s, Extinction ratio is 10.3 dB. (c)Data rate is 25 Gb/s, Extinction ratio is 6.25 dB.

5. Conclusion

The paper summarises the recent our work 2 µm silicon high-speed modulators. By a dedicated 2 µm design, we improved significantly over the previous state-of-the-art 2 µm silicon modulator [5] by achieving: much lower insertion loss (4.96 dB with 2 mm phase shifter vs previous 13 dB 1.5 mm phase shifter), higher data rate (25 Gbit/s vs previous 20 Gbit/s) and higher extinction ratio at the same data rate (10.3 dB at 20 Gbit/s vs previous 5.8dB at 20 Gbit/s).

Acknowledgment

EPSRC (National Hub in High Value Photonic Manufacturing EP/N00762X/1, CORNERSTONE EP/L021129/1); Royal Society (D. J. Thomson Fellowship UF150325); RAEng (M. Nedeljkovic fellowship RF201617/16/33).

References

1. A. Ellis *et al.*, “Capacity in fiber optic communications-the case for a radically new fiber,” in *IEEE Photonic Society 24th Annual Meeting*. IEEE, oct 2011.
2. E. Desurvire *et al.*, “Science and technology challenges in XXIst century optical communications,” *Comptes Rendus Physique*, vol. 12, no. 4, pp. 387–416, may 2011.
3. R. Soref, “Group IV photonics: Enabling 2 µm communications,” *Nature Photonics*, vol. 9, no. 6, pp. 358–359, may 2015.
4. J. J. Ackert *et al.*, “High-speed detection at two micrometres with monolithic silicon photodiodes,” *Nature Photonics*, vol. 9, no. 6, pp. 393–396, may 2015.
5. W. Cao *et al.*, “High-speed silicon modulators for the 2µwavelength band,” *Optica*, vol. 5, no. 9, p. 1055, aug 2018.
6. M. Nedeljkovic *et al.*, “Free-carrier electrorefraction and electroabsorption modulation predictions for silicon over the 1-14-µm infrared wavelength range,” *IEEE Photonics J.*, vol. 3, no. 6, pp. 1171–1180, dec 2011.
7. A. B. Fallahkhair *et al.*, “Vector finite difference modesolver for anisotropic dielectric waveguides,” *Journal of Lightwave Technology*, vol. 26, no. 11, pp. 1423–1431, jun 2008.
8. D. J. Thomson *et al.*, “High performance mach-zehnder-based silicon optical modulators,” *IEEE Journal of Selected Topics in Quantum Electronics*, vol. 19, no. 6, pp. 85–94, nov 2013.